

Probabilistic Modeling of Action Potential Generation by Neurons

Student: Bobby Sena
under the direction of
Professors Helen Wearing and
Eric Toolson
University of New Mexico
bsena@unm.edu

May 6, 2010

Abstract

The function of many cells and organs in the body is absolutely dependent on their ability to generate an electrical signal termed an action potential. The action potential represents a temporal sequence of changes in the electrical potential across a local domain of a cell's plasma membrane, and results from a carefully coordinated sequence of changes in membrane conductance for sodium and potassium ions. We present a model of the dynamical behavior of the gated sodium ion channel, which determines the event of an action potential. Our model is based on the electrical properties of parallel RC circuits, but improves on most current models because it incorporates time- and membrane-potential dependent probabilities that the gated sodium ion channel is in one of three states: closed, open, or inactive. More importantly, our model accounts for the so-called membrane threshold, which is the membrane potential at which the sequence of changes in conductance commences.

Introduction

Neurons are the functional units of the nervous system in multicellular animals. Generally, there are three types of neurons: *sensory neurons*, which communicate information from external stimuli or respond to internal processes within the body, *interneurons*, which communicate signals between other neurons in the nervous system, and *motor neurons*, which send signals toward effectors, such as muscles or glands. These different types of neurons are named according to their functional roles. Neurons communicate instructions in the form of electrical signals, which are called *action potentials*. Most neurons are composed of three functionally distinct areas or regions: the *soma*, which is the main cell-body where most of the vital metabolic processes occur, the *dendrites*, which are fiber-like processes that extend from the soma in multiple directions, and an *axon*, which is also fiber-like and extends from the neuron. Action potentials are generated and carried along the axon.

The neuronal membrane is composed of a phospholipid bilayer, which isolates the intracellular fluid from the extracellular fluid. In general, the phospholipid bilayer is impermeable to ions. However, protein channels embedded in the membrane can facilitate the diffusion of particular ions across the phospholipid bilayer. An important class of these ion channels are those whose conformation depends on the membrane potential. These protein channels are called voltage-gated ion channels, which play a key role in the ability of a neuron to generate and propagate an action potential.

Voltage-gated ion channels are selectively permeable to cations such as sodium (Na^+) and potassium (K^+), see figure 1. Cations that can diffuse across the phospholipid bilayer charge and discharge the intracellular and extracellular fluids. In general, these fluids maintain their respective concentrations of anions. Separation of the charged extracellular and intracellular fluids provides a formal electrical capacitor in the form of the phospholipid bilayer. Cations that can diffuse through the voltage-gated ion channels induce an electrical current¹ across the membrane. The direction of diffusion for a given ionic specie through a voltage-gated ion channel is typically governed by its intracellular-extracellular concentration gradient. However, ions may diffuse through voltage-gated ion channels only

¹This contrasts with the conventional view of electrical current, which is the flow of electrons

when there exists the necessary voltage across the membrane for the channel to open. Hence, voltage-gated ion channels provide variable resistance to the diffusion of ions across the membrane. We may view a localized portion of the phospholipid bilayer as a resistor-capacitor circuit in series, wherein the voltage-gated ion channels represent variable resistors to the current induced by the diffusion of cations.

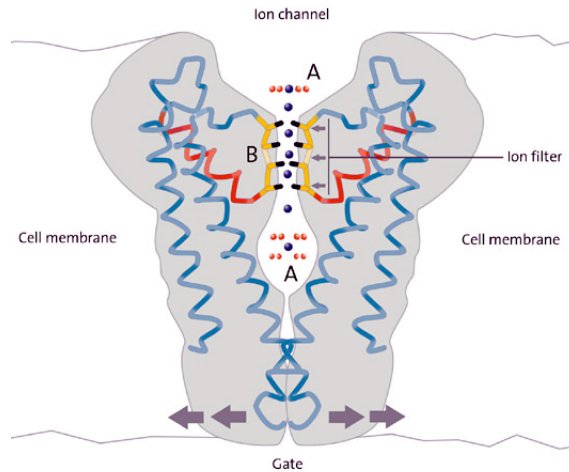


Figure 1: Diagram of potassium voltage-gated channel.

The Hodgkin-Huxley equivalent circuit model of the plasma membrane

Through *voltage-clamping*² techniques, Hodgkin *et al.*, 1952, were able to maintain a constant voltage across the phospholipid bilayer of the giant axon in the squid, or *loligo*, and rapidly step the voltage across the membrane away from its resting potential. They placed the squid giant axon in either sodium- or potassium-saturated solutions and measured the current across the membrane that was required to maintain the voltage step. They provided evidence [4] to suggest that the currents they measured across the cellular membrane were carried by the sodium and potassium cations. Similarly, they measured a “leakage” current carried by other miscellaneous cations such as calcium (Ca^+), which constantly diffuse across the membrane at all membrane potential values. They asserted that these currents were specific to each specie(s) of ion. These currents are collectively represented as

$$I_{\text{ions}} = I_{\text{Na}} + I_{\text{K}} + I_{\text{L}} \quad (1)$$

With their data, they asserted that the permeability of the membrane to either sodium or potassium could be measured by the ratios $I_{\text{Na}}/(V - V_{\text{Na}})$ and $I_{\text{K}}/(V - V_{\text{K}})$, where I_{Na} and I_{K} represent the current carried by the sodium and potassium ions, respectively. V_{Na} and V_{K} represent the equilibrium potentials for which there is no charge transfer due to sodium and potassium ions, respectively. Since these ratios have dimensions equivalent to those for electrical conductance, Hodgkin *et al.*, referred to

$$g_{\text{Na}} = I_{\text{Na}}/(V - V_{\text{Na}}) \quad (2)$$

$$g_{\text{K}} = I_{\text{K}}/(V - V_{\text{K}}) \quad (3)$$

as the conductances of the membrane for sodium and potassium ions, respectively.

In 1952, Hodgkin and Huxley [3] proposed that several resistors and capacitors in parallel could locally model the phospholipid bilayer. Their proposed RC-circuit diagram is shown in figure 2. The diagonal arrows through the resistors in figure 2, which are denoted as R_{Na} , R_{K} , and R_{L} , represent the resistance to the diffusion of Na^+ , K^+ , and miscellaneous other cations.

²Hodgkin *et al.*, threaded a glass micro-pipette down the giant axon of *loligo* (approx. 1mm diameter), and in turn threaded a metal wire through the pipette, which allowed them to measure the voltage (mV) across the membrane. With the axon bathed in ionic solution, they connected the intracellular wire with an extracellular wire through a voltage amplifier. They then abruptly stepped the voltage across the membrane away from resting and measured the current required to maintain that voltage (or oppose) across the membrane.

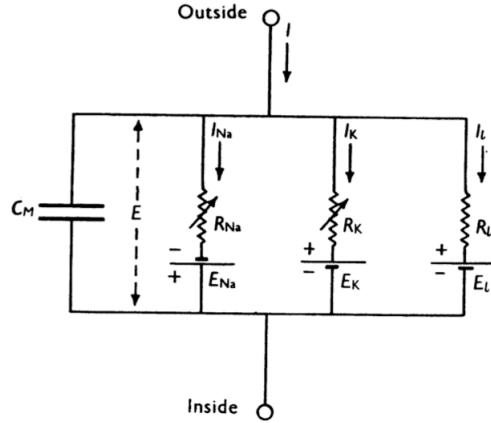


Figure 2: Circuit diagram used by Hodgkin and Huxley[3] to represent neuronal membrane.

Hodgkin-Huxley model of the action potential

In [4], Hodgkin *et al.*, observed a particular potential across the membrane that acted as a threshold for the generation of action potentials. At and beyond this *threshold potential*, the neuron would irreversibly generate an action potential down the axon. This threshold potential is induced by a threshold current. During an action potential, they observed a rapid increase in sodium conductance that was followed by a similar increase in potassium conductance. However, the increase in potassium conductance followed a longer time scale than the increase in sodium conductance. Furthermore, they noted that these increases in conductance values correlated with distinct phases in the membrane potential during an action potential.

First, they observed that the rapid increase in sodium conductance did not occur unless the membrane was depolarized to or beyond its threshold potential. They suggested that this rapid increase in sodium conductance governed the rapid depolarization of the membrane to some peak-potential above zero. Upon approaching the peak-potential, there was a rapid decrease in sodium conductance. At the peak-potential value, there was no sodium conductance.

Similarly, there was an increase in potassium conductance at the onset of an action potential, however it followed a much slower time course than that for the sodium conductance. Hodgkin *et al.*, suggested that the increase in potassium conductance governed with the repolarization of the membrane. The increase in potassium conductance was observed to continue until just after the onset of decreasing sodium conductance. This decrease in potassium conductance continued until the membrane became *hyperpolarized*, that is, until the membrane was polarized below the resting potential. This phase of an action potential is called the *absolute refractory period*. During this time, the membrane cannot become depolarized once again until it has been hyperpolarized. Upon hyperpolarization, there was no conductance for either ion. After hyperpolarization, they observed a gradual return to the resting potential from its hyperpolarized value, which is referred to as the *relative refractory period* of the action potential.

In the absence of a threshold current, no action potential was generated by the neuron. If they innervated the membrane with a sub-threshold current, there would be a slight perturbation in the membrane potential in amplitude less than the threshold potential. Given a sub-threshold current, there was a local response in there was a non-propagated local response to revert the membrane potential back to its resting value. This threshold dynamic is characteristic of the passive electrical properties of the neuron. The generation of action potential exemplifies its active electrical properties. It is now understood that the threshold potential is actually an activating factor for the sodium voltage-gated channel.

Hodgkin and Huxley set out in [3] to generate a mathematical model to account for the dynamics they observed with their voltage-clamp apparatus. Based on their data, Hodgkin and Huxley assumed that the sodium conductance, g_{Na} , obeys a first order differential equation:

$$g_{Na} = \bar{g}_{Na} m^3 h \quad (4)$$

where $\bar{g}_{Na} \equiv 120 \text{ mS/cm}^2$ is taken as a constant, as determined by data.

Biologically, the variable m was assumed to represent some proportion of “activation particles” on the inside of the membrane that become activated by the threshold potential, and allow for the diffusion of sodium ions across the phospholipid bilayer intracellularly. The rapid rise in sodium conductance is modeled by m^3 . The cubic power of m was necessary to fit trends in the rise in sodium conductance. Similarly, h was assumed to represent a proportion

of “inactivation particles” on the outside of the membrane. The singular power of h in 4 was chosen to model the decrease in sodium conductance upon approaching the peak-membrane potential. m and h are collectively referred to as *gating variables*.

Furthermore, m and h were assumed to obey first order differential equations as follows:

$$\frac{dm}{dt} = \alpha_m(1 - m) - \beta_m, \quad (5)$$

$$\frac{dh}{dt} = \alpha_h(1 - h) - \beta_h \quad (6)$$

where $\alpha_{m,h}$ and $\beta_{m,h}$ represent the transfer rates of sodium ions in either direction across the phospholipid bilayer. They are assumed to be functions of voltage of the forms:

$$\alpha_m = 0.1 [25 - (V - V_{eq})] / \left[\exp \frac{25 - (V - V_{eq})}{10} - 1 \right] \quad (7)$$

$$\beta_m = 4 \exp [(V_{eq} - V)/18] \quad (8)$$

$$\alpha_h = 0.07 \exp [(V - V_{eq})/20] \quad (9)$$

$$\beta_h = 1 / \left[\exp \frac{30 - (V - V_{eq})}{10} + 1 \right] \quad (10)$$

where V_{eq} represents the resting potential.

Similarly, to agree with their data, Hodgkin and Huxley assumed that the potassium conductance was proportional to some activation variable, n , which obeyed a fourth power rule to account for the dynamics observed in g_K . They proposed that g_K was of the form:

$$g_K = \bar{g}_K n^4, \quad (11)$$

Furthermore, they assumed that the activation variable n , obeyed the first order differential equation

$$\frac{dn}{dt} = \alpha_n(1 - n) - \beta_n \quad (12)$$

where

$$\alpha_n = 0.01 [10 - (V - V_{eq})] / \left[\exp \left[\frac{10 - (V - V_{eq})}{10} \right] - 1 \right] \quad (13)$$

$$\beta_n = 0.125 \exp [(V_{eq} - V)/80] \quad (14)$$

From their data, they determined that \bar{g}_K is a constant such that $\bar{g}_K \equiv 36 \text{ mS/cm}^2$.

Lastly, Hodgkin and Huxley determined that there is a constant conductance, $g_L \equiv \bar{g}_L$, for many ions through the membrane. The resulting value was taken to be $\bar{g}_L \equiv 0.3 \text{ mS/cm}^2$, which fit with their data.

Equations for membrane potential

With the conductances outlined for each ion of interest, the equations for the Hodgkin-Huxley circuit diagram are derived as follows: Given some charge, Q , across a capacitor, e.g., the lipid bilayer, we have

$$Q = C_m V \quad (15)$$

where C_m is the capacitance of the membrane and V is the voltage, or potential, across the membrane. Since there is a negligible change in the concentrations of sodium and potassium ions in the extracellular and intracellular fluids, C_m is taken to be constant.

From the definition of current, we have that the capacity current, I_c , is given by

$$\begin{aligned} I_c &= \frac{dQ}{dt} \\ &= \frac{d(C_m V)}{dt} \\ &= C_m \cdot \frac{dV}{dt} \end{aligned} \quad (16)$$

Hodgkin and Huxley proposed that the total membrane current, which we will denote I_M , was the sum of the capacitance current and the ionic current, i.e.,

$$I_M = I_c + I_{\text{ions}} \quad (17)$$

$$= C_M \cdot \frac{dV}{dt} + I_{\text{ions}} \quad (18)$$

where this expression we obtain 18 by substitution of 16 into 17.

The resistance for any ionic species X is equal to the inverse of its conductance, g_X , for that specie, i.e., $R = \frac{1}{g_X}$. Ohm's law gives the voltage drop, $\Delta V = (V_{\text{eq}} - V_X)$, induced by an ionic current, I_X , is $(V - V_X) = I_X \cdot R_X$. Hence, solving for I_X gives

$$\begin{aligned} I_X &= \frac{(V - V_X)}{R_X} \\ &= \frac{(V - V_X)}{\frac{1}{g_X}} \\ &= g_X \cdot (V - V_X) \end{aligned} \quad (19)$$

From 19 we have

$$I_{\text{Na}} = g_{\text{Na}} \cdot (V - V_{\text{Na}}) \quad (20)$$

$$I_{\text{K}} = g_{\text{K}} \cdot (V - V_{\text{K}}) \quad (21)$$

$$I_{\text{L}} = g_{\text{L}} \cdot (V - V_{\text{L}}) \quad (22)$$

Kirchhoff's laws for currents that meet at any junction provides that their sum must equal zero. Hence, 18, 1 and 20 - 22 provide

$$\begin{aligned} I_M &= C_M \cdot \frac{dV}{dt} + I_{\text{ions}} \\ &= C_M \cdot \frac{dV}{dt} + I_{\text{Na}} + I_{\text{K}} + I_{\text{L}} \\ &= C_M \cdot \frac{dV}{dt} + g_{\text{K}}(V - V_{\text{K}}) + g_{\text{Na}}(V - V_{\text{Na}}) + g_{\text{L}}(V - V_{\text{L}}) \end{aligned} \quad (23)$$

Conventionally, I_M is considered to be the induced current from voltage-clamping, i.e., an applied current, which we denote I_{applied} . With this in mind, we rearrange equation 23 and solve for $\frac{dV}{dt}$ as follows:

$$\begin{aligned} \frac{dV}{dt} &= (1/C_M) [-g_{\text{K}}(V - V_{\text{K}}) - g_{\text{Na}}(V - V_{\text{Na}}) - g_{\text{L}}(V - V_{\text{L}}) + I_{\text{applied}}] \\ &= (1/C_M) [-\bar{g}_{\text{K}}n^4(V - V_{\text{K}}) - \bar{g}_{\text{Na}}m^3h(V - V_{\text{Na}}) - \bar{g}_{\text{L}}(V - V_{\text{L}}) + I_{\text{applied}}] \end{aligned} \quad (24)$$

where in equation 24 we have substituted the full expressions for g_{Na} and g_{K} from equations 4 and 11, respectively. Additionally, we have substituted g_{L} for \bar{g}_{L} .

Equations 5, 6, 12 and 23 constitute the full Hodgkin-Huxley model of four first order differential equations to describe the membrane potential dynamics of a neuron, which we re-list below:

$$\begin{aligned} \frac{dV}{dt} &= (1/C_M) [-\bar{g}_{\text{K}}n^4(V - V_{\text{K}}) - \bar{g}_{\text{Na}}m^3h(V - V_{\text{Na}}) - \bar{g}_{\text{L}}(V - V_{\text{L}}) + I_{\text{applied}}] \\ \frac{dm}{dt} &= \alpha_m(1 - m) - \beta_m, \\ \frac{dh}{dt} &= \alpha_h(1 - h) - \beta_h \\ \frac{dn}{dt} &= \alpha_n(1 - n) - \beta_n \end{aligned}$$

At the time, numerically solving for systems of four differential equations was very difficult. This led to the development of more simplified models, such as the two-dimensional Fitzhugh-Nagumo model [1]. Although the Fitzhugh-Nagumo yields oscillating solutions for the membrane potential that qualitatively mimic the Hodgkin-Huxley model, it does not account for important features such as the membrane potential threshold dynamics. However, contemporary computing power and algorithms provide accessible resources for solving simple systems of ordinary differential equations well beyond the fourth degree.

Sodium voltage-gated channel

In [3] the activation and inactivation parameters n , m , and h , respectively, are not stated as probabilities. However, it is natural to assign probabilities to the conformations of a given voltage-gated channel at a particular point in time. In particular, the sodium voltage-gated channel, for example, has three distinct states: *open*, which is induced by the threshold potential across the membrane; this enables high sodium conductance to produce an action potential, *inactive*, which prevents the membrane from having any sodium conductance, i.e., prevents the propagation of an action potential, and *closed*, which is the state of the voltage-gated channel when it's not open or inactive.

In [5], Keener shows that the Hodgkin-Huxley equations are in fact exact solutions to general Markovian models for conductances in voltage-gated potassium and sodium channels. From above, we see that the conducting states of any voltage-gated ion channel are the open and closed states. The connection in [5] between these conducting states and the Hodgkin-Huxley equations is made in the probability for the channel to be in either conducting state and the activation/inactivation variables, n , m and h . Qualitatively, the correspondence is made so far as both probabilities and the variables n , m , and h are all dimensionless and furthermore, they all take values on $[0, 1]$.

Vandenberg and Bezanilla in [8] proposed a Markovian model for the voltage-gated sodium channel to be in one of nine different states at a given time. They quantified transitional rate constants between these states according to a given membrane potential. Their model, depicted in figure 3 below, is most compatible with the gating current data that they collected for the sodium voltage-gated channel in the squid giant axon.

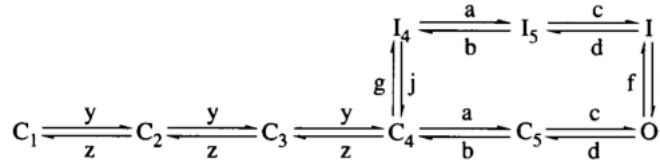


Figure 3: Markovian model proposed in [8].

The proposed conformational states are C_1 , C_2 , C_3 , C_4 , C_5 , I_4 , I_5 , I , and O . It is natural to let O , $C = \sum_{i=1}^5 C_i$, and $I = I + I_4 + I_5$, represent the probability of being open, closed or inactive, respectively. We adopt this approach in our Methods section, where we have denoted the probability of the channel being in the inactive state I , as I for notational convenience.

The addition of four additional closed states to a foundational model including only an open, closed and inactive state, was necessary to fit their data for rate-constants. Similarly, two additional inactive states, I_4 and I_5 were necessary to account for the observed data in which the channel transitioned from a closed state to an inactivated state. Vandenberg and Bezanilla showed that these nine states were necessary and sufficient to account for the ON gating current with and without a rising phase as well as the OFF (inactivation) gating current for the channel. The rate constants between states, which we list below, were best-fit to the data as exponential functions of voltage.

$$y = 16,609 \cdot \exp \left[1.50 \frac{0.22 \cdot V}{24} \right] \quad (25)$$

$$z = 971 \cdot \exp \left[-1.5 \frac{0.78 \cdot V}{24} \right] \quad (26)$$

$$a = 5,750 \cdot \exp \left[0.42 \frac{0.99 \cdot V}{24} \right] \quad (27)$$

$$b = 4,325 \cdot \exp \left[-0.42 \frac{0.01 \cdot V}{24} \right] \quad (28)$$

$$c = 15,669 \cdot \exp \left[1.91 \frac{0.75 \cdot V}{24} \right] \quad (29) \quad 6$$

$$d = 1,361 \cdot \exp \left[-1.91 \frac{0.25 \cdot V}{24} \right] \quad (30)$$

$$f = 432 \cdot \exp \left[0.91 \frac{0.001 \cdot V}{24} \right] \quad (31)$$

$$g = 770 \cdot \exp \left[0.91 \frac{0.001 \cdot V}{24} \right] \quad (32)$$

$$i = 4 \cdot \exp \left[-0.91 \frac{0.999 \cdot V}{24} \right] \quad (33)$$

$$j = \frac{g \cdot i}{f} \quad (34)$$

The probability for the sodium voltage-gated channel to be in any given state at a particular point in time is described by the following first order differential equations:

$$\frac{dO}{dt} = cC_5 + iI - (d + f)O \quad (35)$$

$$\frac{dI}{dt} = cI_5 + fO - (d + i)I \quad (36)$$

$$\frac{dI_5}{dt} = aI_4 + dI - (b + c)I_5 \quad (37)$$

$$\frac{dI_4}{dt} = gC_4 + bI_5 - (j + a)I_4 \quad (38)$$

$$\frac{dC_5}{dt} = aC_4 + dO - (b + c)C_5 \quad (39)$$

$$\frac{dC_4}{dt} = yC_3 + bC_5 + jI_4 - (a + z + g)C_4 \quad (40)$$

$$\frac{dC_3}{dt} = yC_2 + zC_4 - (y + z)C_3 \quad (41)$$

$$\frac{dC_2}{dt} = yC_1 + zC_3 - (y + z)C_2 \quad (42)$$

$$C_1 = 1 - (C_2 + C_3 + C_4 + C_5 + O + I_4 + I_5 + I) \quad (43)$$

Methods

We consider work done by Hodgkin and Huxley in [3], which has proven to be foundational to the study of neurons and actional potentials. Additionally, we seek to expand upon the work done by Vandenberg and Bezanilla in [8] by substituting a dynamic voltage variable, V , into equations 25 - 34 for the static value used in [8]. We propose a system of ten ordinary differential equations, which provide intuitive insight into the Hodgkin-Huxley equations.

Since the state of the sodium voltage-gated channel is voltage-dependent, with the appropriate substitution for V from equation 24 into equations 25 - 33, we have that equations 25 - 34 are now dynamic functions of voltage. This induces voltage dependence in equations 35 - 43. Qualitatively, voltage- and time-dependent membrane state-probabilities are consistent with $g_{Na}(V, t)$ as seen in equation 4. However, we note that time, t , in 24 is measured in milliseconds, so we scale equations 25 - 33, which are measured in seconds, by multiplying the right each right hand side of each equation by 10^{-3} .

We recall that the activation variables, m and h for the sodium voltage-gated channel are dimensionless and take values on the interval $[0, 1]$. Additionally, m and h represent the proportions of some activating molecules on the inside of the membrane and inactivating molecules on the outside of the membrane, respectively. Lastly, the cubic power of m was chosen in [3] to represent the presence of three (assumed) activating molecules on the inside of the membrane. Similarly, the singular power of h was chosen to represent the presence of one inactivating particle on the outside of the membrane³. Hence the product m^3h accounts for the activation and inactivation of the sodium voltage-gated channel, as seen in equation 4.

³These assumptions were made in [3] to account for the rapid activation and much slower inactivation of g_{Na} . It is now understood that such "molecules" do not actually exist, but rather, the dynamics that these variables exhibit are governed by physiological subunits of the sodium voltage-gated channel. This aspect however, is beyond the scope of this study.

We propose a substitution of the solution for O in equation 35 for the product m^3h in 4. This is well defined since $O(V, t)$ is also takes values on $[0, 1]$ and is dimensionless. Conclusively, the probability of the sodium voltage-gated channel being open has already macroscopically accounted for the activation and inactivation dynamics of the channel. Since the generation of an action potential is principally governed by sodium conductance, we feel that this substitution provides a mechanistic approach to capturing the membrane potential dynamics of the neuron during an action potential.

We exhibit our substitution of O for m^3h in equation 24 below:

$$\frac{dV}{dt} = (1/C_M) [-\bar{g}_K n^4 (V - V_K) - \bar{g}_{Na} O (V - V_{Na}) - \bar{g}_L (V - V_L) + I_{\text{applied}}] \quad (44)$$

Our proposed model in full is the series of equations 12, 35 - 43, and 44 as follows:

$$\begin{aligned} \frac{dO}{dt} &= cC_5 + iI - (d + f)O & \frac{dC_5}{dt} &= aC_4 + dO - (b + c)C_5 \\ \frac{dI}{dt} &= cI_5 + fO - (d + i)I & \frac{dC_4}{dt} &= yC_3 + bC_5 + jI_4 - (a + z + g)C_4 \\ \frac{dI_5}{dt} &= aI_4 + dI - (b + c)I_5 & \frac{dC_3}{dt} &= yC_2 + zC_4 - (y + z)C_3 \\ \frac{dI_4}{dt} &= gC_4 + bI_5 - (j + a)I_4 & \frac{dC_2}{dt} &= yC_1 + zC_3 - (y + z)C_2 \end{aligned}$$

$$C_1 = 1 - (C_2 + C_3 + C_4 + C_5 + O + I_4 + I_5 + I)$$

$$\begin{aligned} \frac{dV}{dt} &= (1/C_M) [-\bar{g}_K n^4 (V - V_K) - \bar{g}_{Na} O (V - V_{Na}) - \bar{g}_L (V - V_L) + I_{\text{applied}}] \\ \frac{dn}{dt} &= \alpha_n (1 - n) - \beta_n \end{aligned}$$

with rate constants from [8], which are now all functions of voltage:

$$\begin{aligned} y &= 10^{-3} \cdot 16,609 \cdot \exp \left[1.50 \frac{0.22 \cdot V}{24} \right] & d &= 10^{-3} \cdot 1,361 \cdot \exp \left[-1.91 \frac{0.25 \cdot V}{24} \right] \\ z &= 10^{-3} \cdot 971 \cdot \exp \left[-1.5 \frac{0.78 \cdot V}{24} \right] & f &= 10^{-3} \cdot 432 \cdot \exp \left[0.91 \frac{0.001 \cdot V}{24} \right] \\ a &= 10^{-3} \cdot 5,750 \cdot \exp \left[0.42 \frac{0.99 \cdot V}{24} \right] & g &= 10^{-3} \cdot 770 \cdot \exp \left[0.91 \frac{0.001 \cdot V}{24} \right] \\ b &= 10^{-3} \cdot 4,325 \cdot \exp \left[-0.42 \frac{0.01 \cdot V}{24} \right] & i &= 10^{-3} \cdot 4 \cdot \exp \left[-0.91 \frac{0.999 \cdot V}{24} \right] \\ c &= 10^{-3} \cdot 15,669 \cdot \exp \left[1.91 \frac{0.75 \cdot V}{24} \right] & j &= \frac{g \cdot i}{f} \end{aligned}$$

The values for V_{Na} and V_K have been provided in [3]. In accordance with [3], we determine V_L such that the total current across the membrane is zero at the resting potential, V_{eq} , i.e., we solve equation 44 for V_L when $I_{\text{applied}} \equiv 0$, which gives:

$$V_L = V_{\text{eq}} + (1/C_m) [\bar{g}_K n_0^4 (V_{\text{eq}} - V_K) + O_{\text{steady-state}} \bar{g}_{Na} (V_{\text{eq}} - V_{Na})], \quad (45)$$

where n_0 is the steady state value for n , which is defined in [3] as

$$n_0 = \frac{\alpha_{n_0}}{\alpha_{n_0} + \beta_{n_0}} \quad (46)$$

for $\alpha_{n_0} = \alpha_n(V_{\text{eq}})$ and $\beta_{n_0} = \beta_n(V_{\text{eq}})$ from 13 and 14, respectively.

However, the solution to equation 45 requires a steady state value, $O_{\text{steady-state}}$, for equation 35. We determine the steady-state values for equations 35 - 42 by solving the system of linear equations that results from calculating the values for 25 - 34 when $V \equiv V_{\text{eq}}$, for some fixed value of V_{eq} . This reduces to solving for the vector x in $\dot{x} = Ax + B$ when $\dot{x} \equiv 0$. We illustrate $\dot{x} = Ax + B$ below⁴:

$$\underbrace{\begin{bmatrix} \frac{dO}{dt} \\ \frac{dI}{dt} \\ \frac{dI_5}{dt} \\ \frac{dI_4}{dt} \\ \frac{dC_5}{dt} \\ \frac{C_4}{dt} \\ \frac{dC_3}{dt} \\ \frac{dC_2}{dt} \end{bmatrix}}_{\dot{x}} = \underbrace{\begin{bmatrix} -(d+f) & i & 0 & 0 & c & 0 & 0 & 0 \\ f & -(d+i) & c & 0 & 0 & 0 & 0 & 0 \\ 0 & d & -(b+c) & a & 0 & 0 & 0 & 0 \\ 0 & 0 & b & -(j+a) & 0 & g & 0 & 0 \\ d & 0 & 0 & 0 & -(b+c) & a & 0 & 0 \\ 0 & 0 & 0 & j & b & -(a+z+g) & y & 0 \\ 0 & 0 & 0 & 0 & 0 & z & -(y+z) & y \\ -y & -y & -y & -y & -y & -y & (z-y) & -(2y+z) \end{bmatrix}}_A \underbrace{\begin{bmatrix} O \\ I \\ I_5 \\ I_4 \\ C_5 \\ C_4 \\ C_3 \\ C_2 \end{bmatrix}}_x + \underbrace{\begin{bmatrix} 0 \\ 0 \\ 0 \\ 0 \\ 0 \\ 0 \\ 0 \\ y \end{bmatrix}}_B \quad (47)$$

We solve for x when 47 is set to zero using MATLAB's "backslash" operator, which performs left-division for matrices, i.e., we solve the equation

$$x = A^{-1}(-B) \quad (48)$$

We illustrate this process in appendix A.

For a given resting potential, V_{eq} , we numerically solve for the membrane potential and channel state probabilities for steps in applied current, I_{applied} , from 0 up to $50 \mu\text{A}/\text{cm}^2$. Lastly, we plot our results on axes for probability against time, and membrane potential, in millivolts, against time, which we measure in milliseconds. We obtain our results utilizing one of MATLAB's stiff ODE-solvers, ode23s, specifying initial conditions for the sodium channel state-probabilities as outlined in [8]. We specify all other initial conditions as determined by solutions to equation 48. Our source code is provided in appendix B. We compare our results for membrane potential with those from [3].

Results

Numerical simulation of our model for steps in applied current, I_{applied} , yields characteristic membrane potential dynamics. Most importantly, our model exhibits threshold dynamics, as shown in figure 4. We plot our results for membrane potential and channel state-probabilities in figures 8(a) and 8(b), respectively. In addition to threshold dynamics, we observe and identify distinct characteristic features of action potentials. Lastly, we find biologically significant behavior in the state-probabilities of the Na^+ channel during an action potential.

Membrane potential dynamics

We see that in the absence of any applied current, there is no perturbation in the membrane potential, see figure 5(a). Second, given a sub-threshold current, there is a slight upward perturbation in the membrane potential. This is countered by a local response, which repolarizes the membrane to its resting potential. In particular, we note that if the membrane potential is not depolarized to its threshold value, there is no action potential.

We approximate a threshold current value of around $5 \mu\text{A}/\text{cm}^2$ by investigation of figure 4. At or above this value, there is depolarization in the membrane potential beyond its threshold value, and we observe action potential behavior. This behavior is identified by a rapid depolarization with overshoot beyond 0 mV, up to a maximum value that is below the equilibrium voltage, V_{Na^+} , for Na^+ . The duration of depolarization is approximately 2ms. Furthermore, the duration of depolarization occurring beyond the threshold potential and up to the peak-value is shorter than the duration of depolarization up to the threshold potential.

During the absolute refractory period after the peak, repolarization of the membrane undershoots the resting potential by approximately 5-10 mV. The absolute refractory period proceeds for a duration of time that is approximately three times longer than that of the entire depolarization period. The hyperpolarized membrane potential does not reach the equilibrium potential, V_{K} , for potassium.

⁴For convenience, we do not include C_1 since it is a linear combination of 35 - 42.

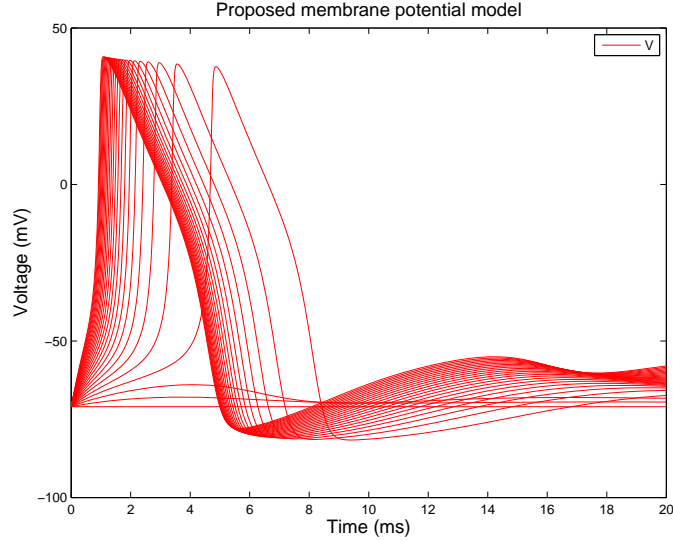
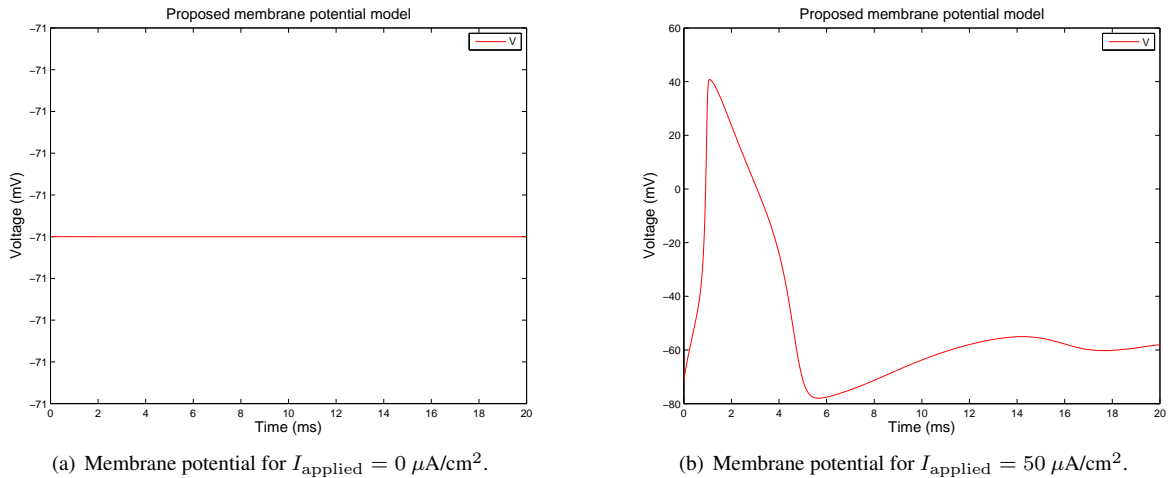


Figure 4: Channel state probabilities for steps in applied current, I_{applied} , from 0 - 50 $\mu\text{A}/\text{cm}^2$ in increments of 2.

Lastly, we see that the relative refractory period after hyperpolarization returns the membrane to a stable potential. We note however, that this stable potential is above the initial resting potential for the membrane. Additionally, there are slight oscillations during stabilization. The time duration for the relative refractory period is at least twice as long as the depolarization and hyperpolarization periods combined.



(a) Membrane potential for $I_{\text{applied}} = 0 \mu\text{A}/\text{cm}^2$.

(b) Membrane potential for $I_{\text{applied}} = 50 \mu\text{A}/\text{cm}^2$.

Figure 5: Membrane potential for Na^+ channel.

Channel state-probability dynamics

Solutions to the state-probabilities for the Na^+ channel are qualitatively consistent with the dynamics of the membrane potential. First, in the absence of any applied current, there are steady state values for O , C , and I . Additionally, there is a low probability of the channel being inactive as well as no probability of the channel being open. These results are seen in figure 6(a).

Simulating some applied current at or above threshold yields fluctuations in the channel state-probabilities. First, there is a rapid decline in the probability of the sodium voltage-gated channel being closed. This correlates with a rapid increase in the probability of the channel being open from a value of zero. We note a gradual increase in the probability

of the channel being inactive. Finally, the probabilities I and C stabilize around an split of values approaching 0.5. There is a concurrent digression of probability O to zero. These dynamics are seen in figure 6(b).

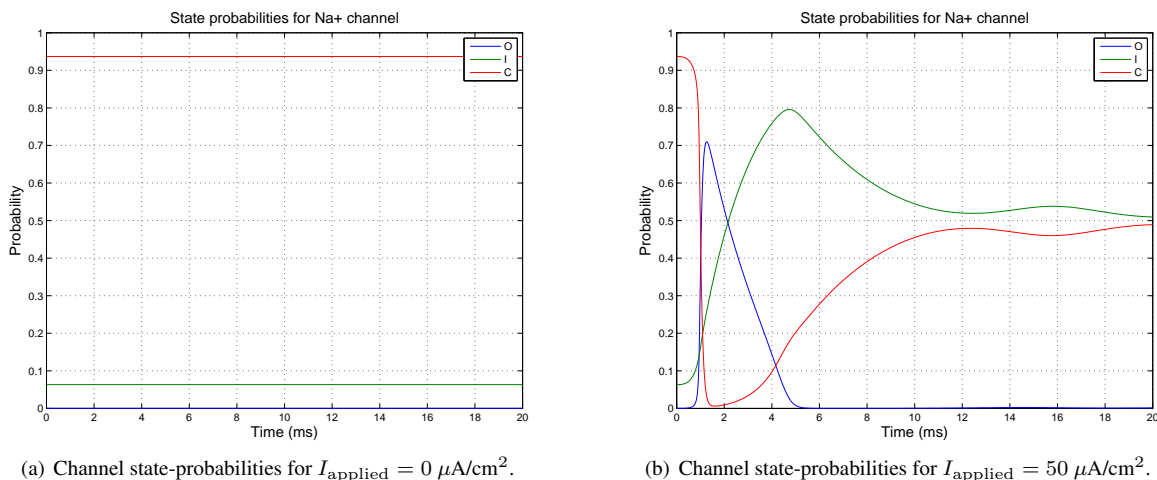


Figure 6: Channel state-probabilities for Na⁺ channel.

Discussion

We have presented a system of ten ordinary differential equations to model membrane potential dynamics in neurons, and in particular, action potential generation by neurons. We have expanded upon work done by Vandenberg and Bezanilla in [8] by accounting for a dynamic membrane potential in our calculations of their proposed rate constants as seen in equations 25 - 34. We incorporated these results with the foundational work done by Hodgkin and Huxley in [3] by substituting the two sodium conductance activation and inactivation variables, m and h , respectively, for a single variable, O , which represents the probability of a sodium voltage-gated channel being in an open, or conducting, conformation, which we obtained from [8]. We discuss two aspects of our model that seem promising. First, we obtained plots for action potentials that are comparable with those obtained from the Hodgkin-Huxley equations. Second, our results for calculated state-probabilities for the sodium voltage-gated channel are qualitatively consistent with our results for membrane potential during an action potential.

Comparison of proposed model to Hodgkin-Huxley model

Since this study was largely motivated by the robustness of the Hodgkin-Huxley model put forth in [3], it is fitting to use their results as a benchmark for our success. Upon simulating results from [3] in MATLAB under identical conditions to our simulation of our own model, we have the two plots depicted in figure 7. At a glance, our results are qualitatively consistent with those from [3]. We note however, that the action potential generated by our model is of smaller amplitude than that for the Hodgkin-Huxley model. We suggest that this largely due to the fact that our channel never exhibits a fully open state, as seen in figure 6(b). This of course is a consequence of the rate constants proposed in [8].

Additionally, the relative refractory period of our action potential oscillates around a stable-state potential that is above the initially specified equilibrium potential at rest. This contrasts with the relative refractory period depicted in figure 7(a) for [3], which monotonically converges to the resting potential. We infer that this is most likely due to our consideration of the large number of nonlinear equations that comprise the rate constants in [8], which are all exponential functions of voltage. This could also be due to the machine precision that was introduced at the solution to equation 48 via MATLAB's backslash operator, since all of our steady-state solutions take values on the interval (0,1).

Perhaps most important is the lack of a distinct threshold potential in figure 7(b). We note however, that there is a slight inflection point in the membrane potential at around -40mV, which is slightly below the corresponding value

in figure 7(a). If we recall evidence for the threshold potential from figure 4, we see that the threshold potential is actually closer to -60mV . This could be due to some predisposition of the membrane to being open, although that is perhaps least likely since values for C and I in figure 6(b) tend to be greater than O on average.

Additionally, we observe a lower hyperpolarized value for our model. This be due in part by what seems to a predisposition to be in a closed state by the sodium voltage-gated channel, which we observe figure 6. Physiologically, this would correspond to a potassium conductance-constant value \bar{g}_K that is too high. This is likely if we consider possible discrepancies in the experimental techniques of [8] against those of [4].

Lastly, we observe that the spike in the action potential in figure 7(b) is wider than that from [3]. This could mean our substitution had some adverse affect on the time scale for potassium conductance. However, Hodgkin and Huxley assert in [3] that this is perhaps more representative of actual data than a more pointed spike for some cases of neuron.

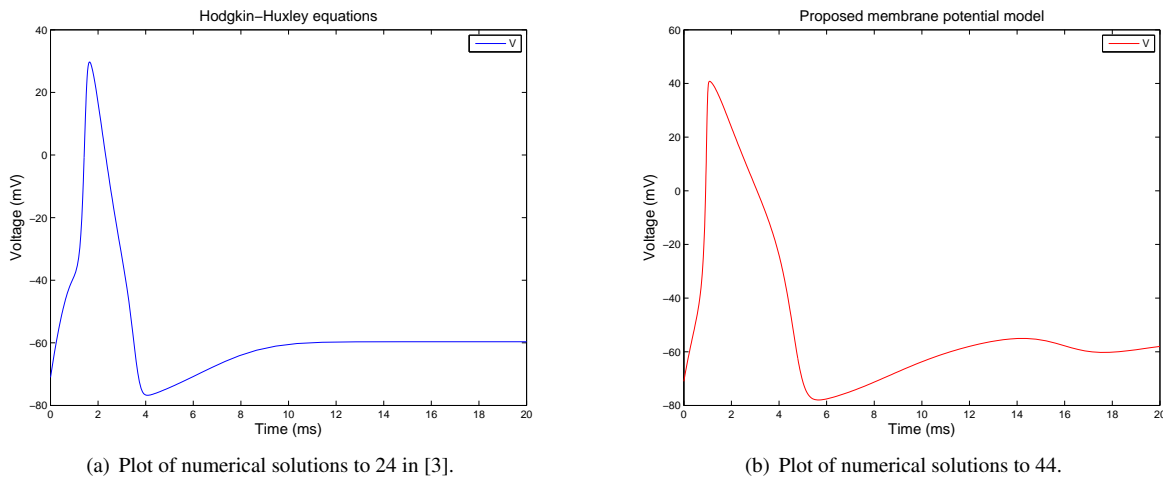


Figure 7: Comparison of results from [3] with those of our proposed model.

Proposed model simulation for membrane potential

Due to its richness in distinct and qualifying features for an action potential, we feel that our model captures most of the key aspects of the Hodgkin-Huxley model. We note that our model is incomplete however, in that it does not explicitly account for probabilistic processes for the potassium voltage-gated channel. However, our model does provide comparable results to the Hodgkin-Huxley model by utilizing what is perhaps a more intuitive approach by utilizing conformational state probabilities for the one channel that determines the eventuation of an action potential.

Proposed model simulation for channel state-probabilities

Our model does a good job in correlating the conformational state probabilities for the sodium channel with distinct phases in an action potential. This is evident in figure 8. First, we see that the depolarization phase correlates to a rapid increase in the probability of the sodium channel being open. Simultaneously, this the probability of the channel being in an closed state tends toward zero. We observe that as the membrane potential reaches its peak value, there is an inflection point in the O curve, which approaches zero thereafter.

We notice that the onset of the increase in O corresponds to an increase in I , which reaches its peak value later than O . The maximum I value also shortly precedes the hyperpolarized potential. This is consistent with known dynamics of the sodium voltage-gated channel.

Appendices

A

```
function [X] = steadystate(veq)

%=====
scale=10^(-3); %scale time to agree with Hodgkin-Huxley
5
%=====RATE CONSTANTS=====
y=scale*16609*exp(1.5*(0.22*veq)/24);
z=scale*971*exp(-1.5*(0.78*veq)/24);
a=scale*5750*exp(0.42*(0.99*veq)/24);
10 b=scale*4325*exp(-0.42*(0.01*veq)/24);
c=scale*15669*exp(1.91*(0.75*veq)/24);
d=scale*1361*exp(-1.91*(0.25*veq)/24);
f=scale*432*exp(0.91*(0.001*veq)/24);
g=scale*770*exp(0.91*(0.001*veq)/24);
15 h=scale*4*exp(-0.91*(0.999*veq)/24);%i from Vandenberg and Bezanilla
k=(g*h)/f;%j from Vandenberg and Bezanilla
%=====

%=====STEADY-STATE MATRIX PROBLEM=====
20 A=[-(d+f) h 0 0 c 0 0 0;
      f -(d+h) c 0 0 0 0 0;
      0 d -(b+c) a 0 0 0 0;
      0 0 b -(k+a) 0 g 0 0;
      d 0 0 0 -(b+c) a 0 0;
25 0 0 0 k b -(a+z+g) y 0;
      0 0 0 0 0 z -(y+z) y;
      -y -y -y -y -y -y z-y -(2*y+z)]; %matrix of rate-
                                          %constant coefficients

30 B=[0;0;0;0;0;0;0;-y]; %vector of constant terms

X=A\B; %solve for vector, X, of steady-state probabilities
%=====
```

B

```
function []=membranepotential(v,vK,vpass,vNa,...
    gbarK,gbarNa,gm,Cm,Iapplied,tmax,X)

%=====PARAMETER VALUES=====
5 Iapplied=50; %variable
veq=-71; %mV
vK=veq-12; %mV
vNa=veq+115; %mV
X = steadystate(veq);%vector of steady-state probabilities
10 gbarK=36; % (mS/cm^2)
gbarNa=120; % (mS/cm^2)
gm=0.3; % (mS/cm^2)

alphan0=0.01*10/(exp(1)-1); %ms^-1
15 betan0=0.125; %ms^-1
```

```

n0=alphan0/(alphan0+betan0); %dimensionless activation variable
                                %for potassium K^+

vpass=veq+(gbarK*((n0)^4)*(veq-vK)+X(1)*gbarNa*(veq-vNa))/gm; %leakage
                                                                %voltage
20

Cm=1; %membrane capacitance-constant (given)
tmax=20;%maximum time for evaluating membrane potential
%=====
25
%=====SOLVE ODE'S=====
figure(1); clf(1);
[t,x] = ode23s(@(t,x)prob(t,x,Iapplied,vK,veq,vpass,vNa,...
    gbarK,gbarNa,gm,Cm),[0,tmax],...
30 [X;veq;n0]);%solve ODE's for V,n,probability states
%=====

%=====PLOTS=====
35 subplot(2,1,1)
plot(t,x(:,1),t,sum(x(:,2:4)'),t,1-sum(x(:,1:4)'),t,x(:,10).^4) %plot state probability
                                                                %for Na+ channel

legend('O','I','C','n')
xlabel('Time (ms)','FontSize',14)
ylabel('Probability','FontSize',14)
40 title('Probabilities','FontSize',14)
axis([0 tmax 0 1])
grid

subplot(2,1,2)
45 plot(t,x(:,9)) %plot membrane potential against time
legend('V')
xlabel('Time (ms)','FontSize',14)
ylabel('Voltage (mV)','FontSize',14)
x(end,:);
50 %=====

%=====PROBABILITY ODES=====
function [dx] = prob(t,x,Iapplied,vK,veq,vpass,vNa,...
    gbarK,gbarNa,gm,Cm)
55 dx = zeros(10,1);
v(1)=x(9); %substitution for convenience
scale=10^(-3); %scale rate constants to agree
                %with Hodgkin-Huxley time scale

%===parameters as functions of voltage (v)===
60 y=scale*16609*exp(1.5*(0.22*v(1))/24);
z=scale*971*exp(-1.5*(0.78*v(1))/24);
a=scale*5750*exp(0.42*(0.99*v(1))/24);
b=scale*4325*exp(-0.42*(0.01*v(1))/24);
c=scale*15669*exp(1.91*(0.75*v(1))/24);
65 d=scale*1361*exp(-1.91*(0.25*v(1))/24);
f=scale*432*exp(0.91*(0.001*v(1))/24);
g=scale*770*exp(0.91*(0.001*v(1))/24);
h=scale*4*exp(-0.91*(0.999*v(1))/24); %i from Vandenberg and
                                %Bezanilla
70 k=(g*h)/f; %j from Vandenberg and Bezanilla

%alpha & beta values for activation variable n=
alphan=0.01*(10+(veq-v(1)))/(exp((10+(veq-v(1)))/10)-1);
betan=0.125*exp((veq-v(1))/80);

```

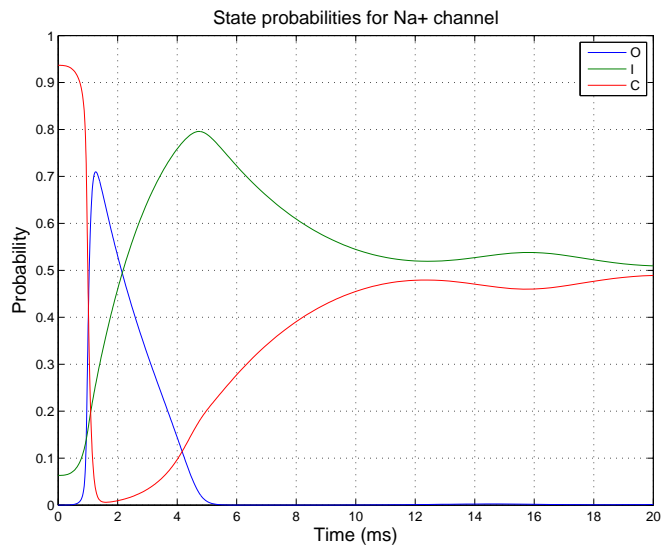
```

75 %==ODE's for Na+ channel state probabilities==
dx(1) = c*x(5)+h*x(2)-(d+f)*x(1); %d0/dt
dx(2) = c*x(3)+f*x(1)-(d+h)*x(2); %dI/dt
dx(3) = a*x(4)+d*x(2)-(b+c)*x(3); %dI5/dt
dx(4) = g*x(6)+b*x(3)-(k+a)*x(4); %dI4/dt
80 dx(5) = a*x(6)+d*x(1)-(b+c)*x(5); %dC5/dt
dx(6) = y*x(7)+b*x(5)+k*x(4)-(a+z+g)*x(6); %dC4/dt
dx(7) = y*x(8)+z*x(6)-(y+z)*x(7); %dC3/dt
dx(8) = y*(1-(x(8)+x(7)+x(6)+x(5)+...
      x(1)+x(4)+x(3)+x(2)))+z*x(7)-(y+z)*x(8); %dC2/dt
85 %=====ODE for membrane potential=====
dx(9) = (-gbarK.*(x(10)^4)*(v(1)-vK)-...
      gbarNa*(x(1))*(v(1)-vNa)...
      -gm*(v(1)-vpass)+Iapplied)/Cm; %dV/dt
dx(10) = alphan.*(1-x(10))-betan.*x(10); %dn/dt
90 %=====

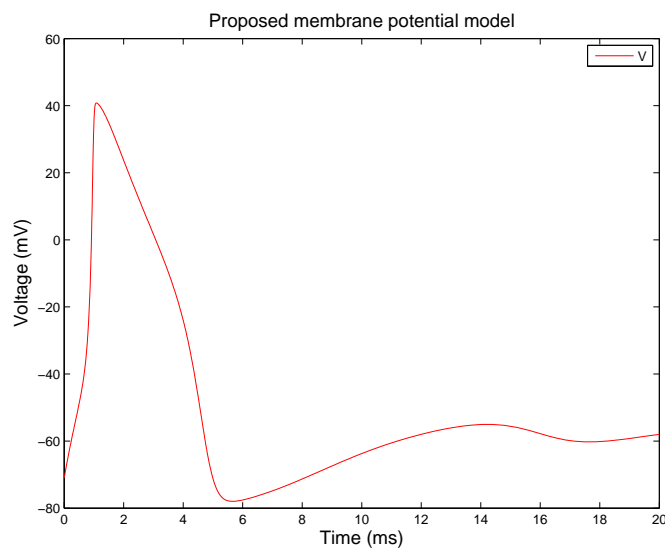
```

References

- [1] [Fitzhugh, R., 19060] Fitzhugh, Richard. 1960. Thresholds and Plateaus in the Hodgkin-Huxley Nerve Equations. *The Journal of General Physiology*, 43: 867-896.
- [2] [Hodgkin, A.L., Huxley, A.F., 1952a] Hodgkin, A.L., and A.F. Huxley. (1952a). Currents carried by sodium and potassium ions through the membrane of the giant axon of *Loligo*. *J. Physiol. (Lond.)*. 116:449-472.
- [3] [Hodgkin, A.L., Huxley, A.F., 1952b] Hodgkin, A.L., and A.F. Huxley. (1952b). A quantitative description of the membrane current and its application to conduction and excitation in nerve. *J. Physiol. (Lond.)*. 117:500-544.
- [4] [Hodgkin, et al., 1952] Hodgkin, A. L., A. F. Huxley and B. Katz. 1952. Measurement of current-voltage relations in the membrane of the giant axon of *Loligo*. *J. Physiol.* 116: 424-448
- [5] [Keener, J. P., 2009] Keener, J.P. 2009. Invariant Manifolds Reductions for Markovian Ion Channel Dynamics. *Journal of Mathematical Biology*. 58:447
- [6] [Keener, J., Sneyd, J., 2009] Keener, J., Sneyd, J. 2009. *Mathematical Physiology I: Cellular Physiology*, 2nd ed. Springer Science+Business Media, LLC, NY, pp. 175-223.
- [7] [Randall, et al., 2002] Randall, D, Warren, G., French, K. 2002. *Eckert Animal Physiology: Mechanisms and Adaptations*, 5th ed. W. H. Freeman and Company, NY, pp. 115 - 151.
- [8] [Vandenberg, C.A., Bezanilla, F., 1991] Vandenberg, C.A., and F. Bezanilla. 1991. A sodium channel gating model based on single channel, macroscopic ionic, and gating currents in the squid giant axon. *Biophys. J.* 60:1511-1533.



(a) State probabilities for Na⁺ channel.



(b) Membrane potential

Figure 8: State probabilities on same time scale as membrane potential.